Water Practice & Technology

IWA PUBLISHING

Water Practice & Technology Vol 19 No 3, 671 doi: 10.2166/wpt.2024.048

Adsorption of the fungicide carbendazim on activated carbon: analysis of isotherms, kinetics, rapid small-scale column tests, and impacts of the presence of organic matter

Ian Rocha de Almeida *, Geovana Eliza Maria Keller, Lígia Conceição Tavares, Salatiel Wohlmuth da Silva and Antônio Domingues Benetti

Hydraulic Research Institute, Federal University of Rio Grande do Sul, 9500 Bento Gonçalves Avenue, Porto Alegre, Rio Grande do Sul, Brazil
*Corresponding author. E-mail: ian.almeida@ifpa.edu.br

IR deA, 0000-0001-6916-3295

ABSTRACT

The adsorption of the fungicide carbendazim (CBZ) on granular activated carbon (GAC) made from bovine bone was investigated in deionized water (DW) and DW with the addition of natural organic matter (DWNOM). The study included tests of isotherms, kinetics, and rapid small-scale column tests (RSSCT). The Freundlich model represented better the adsorption of the fungicide in both matrices, while the pseudo-second-order model fitted better in DW. The isotherm and kinetic studies showed the interference of NOM in the adsorption of CBZ through changes in the parameters of the applied models. In RSSCT, the breakthrough time was faster in DWNOM than in DW. Nevertheless, the CBZ concentrations of both matrices were considered statistically similar for most contact times in RSSCT. In the fixed-bed experiments, the organic matter did not cause significant changes in the adsorption of CBZ in GAC. The NOM presence may have improved the efficiency of GAC in adsorbing CBZ in kinetic and RSSCT tests. There is no knowledge of a similar approach to studying the adsorption of CBZ on GAC in Brazil, mainly using fixed-bed studies. In this way, the present work contributes to a better understanding of the adsorption of carbendazim through the methods used.

Key words: adsorption, carbendazim, isotherms, kinetics, natural organic matter, rapid small-scale column tests

HIGHLIGHTS

- Bovine bone GAC removed carbendazim in deionized water (DW) and deionized water with the addition of natural organic matter (DWNOM).
- Freundlich isotherm and pseudo-second-order equation fitted better the adsorption of CBZ in DW and DWNOM.
- There was a 72% reduction in the Freundlich constant (K_f) of the isotherm with DWNOM compared to DW.
- The interference of NOM was not significant in the adsorption of CBZ on RSSCT.

GRAPHICAL ABSTRACT

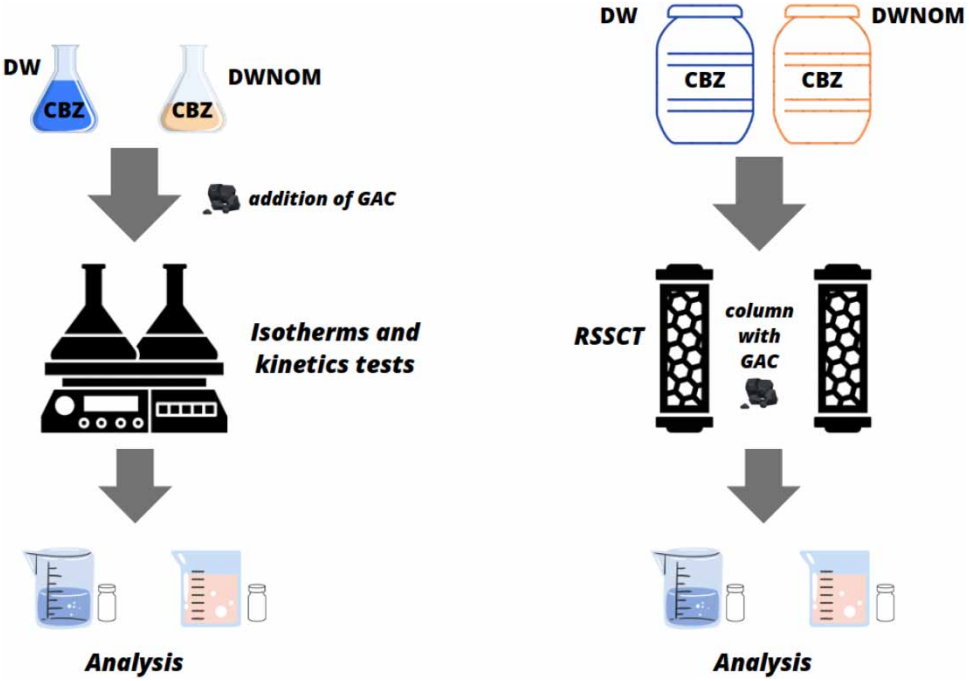

1. INTRODUCTION

Contaminants of emerging concern (CEC) are chemical compounds that can affect human health and the environment. They are present at low concentrations in water bodies, sanitary sewage, and sometimes in treated water for human consumption (WRMA 2019). CECs are released into the environment due to anthropic activities. One of these compounds is pesticides, substances that control pests considered harmful to crops and disease vectors (Kümmerer 2011). The presence of these compounds in the environment has a common origin, mainly agricultural activities. They reach water bodies after being dissolved or adsorbed to soil particles and transported by catchment runoff to surface waters or infiltration to groundwater (Novotny 2002; Sellaoui *et al.* 2023).

Carbendazim (CBZ), a pesticide from the benzimidazole group (Rama *et al.* 2014), is one of Brazil's most widely used pesticides. The Brazilian National Health Surveillance Agency (*Agência Nacional de Vigilância* Sanitária – ANVISA) has banned this compound (ANVISA 2022). However, its elimination is expected to be gradual since Brazilian farmers widely use CBZ in the plantations of beans, rice, soybeans, and other agricultural products (Peduzzi 2022). Figure 1 shows the molecular structure of CBZ.

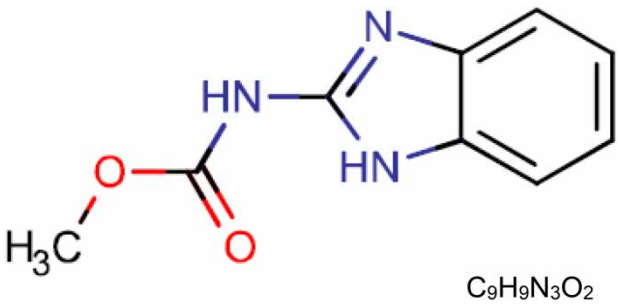

Figure 1 | Chemical structure of carbendazim (Chemicalize 2021).

The toxicological re-evaluation conducted by ANVISA between 2020 and 2022 concluded that the fungicide has carcinogenic potential, induces germ cell mutations, and can cause reproductive toxicity in humans. The agency pointed out that it was not possible to find a safe dose threshold for humans for mutagenicity and

reproductive toxicity characteristics (ANVISA 2022). Carbendazim is on the Norman list of emerging substances with sufficient evidence of risk, requiring the adoption of mitigating measures (Dulio *et al.* 2014).

Several studies evaluated advanced water treatment technologies for removing and controlling health and environmentally harmful CEC, such as CBZ. The adsorption process has been used for several years to produce drinking water and treat domestic wastewater and industrial effluents. Activated carbon is the main adsorbent used for this purpose, both pulverized and granular, the latter being used in fixed beds. Dynamic adsorption (which occurs in fixed beds) can be employed in the removal of natural organic matter (NOM) and CEC, with many studies proving its good performance in reducing these compounds in water (Domergue *et al.* 2022; Sellaoui *et al.* 2023). Several methodologies are employed in analyzing the adsorptive process, such as isotherms and adsorption kinetics. In fixed-bed studies, rapid small-scale column tests (RSSCT) are often used (Crittenden *et al.* 2012).

The adsorption isotherms are essential to evaluate activated carbon's performance in removing a specific adsorbate. They mathematically represent the relationship between the amount of adsorbate extracted by the adsorbent and the amount of adsorbate remaining in the liquid phase when the solution is in equilibrium at a given temperature (Piccin *et al.* 2017). Kinetic models have been used to analyze experimental data to investigate adsorption mechanisms and rates. The most studied models include the pseudo-first-order, the pseudo-second-order, and the intraparticle diffusion models (Ho & Mckay 1998; Haro *et al.* 2021).

RSSCT is one of the most widely used methods for estimating the performance of an activated carbon fixed-bed column. This methodology involves the determination of breakthrough curves and other operating parameters from small-scale tests. Fixed-bed-based mass transfer models are applied to evaluate the performance of granular activated carbon (GAC) at full scale from RSSCT (Crittenden *et al.* 1987). The shape and size of the breakthrough curve depend on several parameters, including adsorption rate, temperature, flow rate, bed length, contaminant concentration, presence of organic matter, and pH (Domergue *et al.* 2022).

Under natural conditions and in treatment plants, NOM can be present in different concentrations. NOM is a complex mixture of organic compounds such as fulvic and humic acids, hydrophilic acids, and specific compounds such as carbohydrates and proteins, all of natural origin (Summers *et al.* 2011). Humic acids are the main constituents of NOM in natural waters. They are rich in aromatic carbon, phenolic structures, and conjugated double bonds (Figure 2), with molecular weight ranging from 500 to more than 10,000 (Thurman *et al.* 1982; Duan & Gregory 2003; Silanpää 2015).

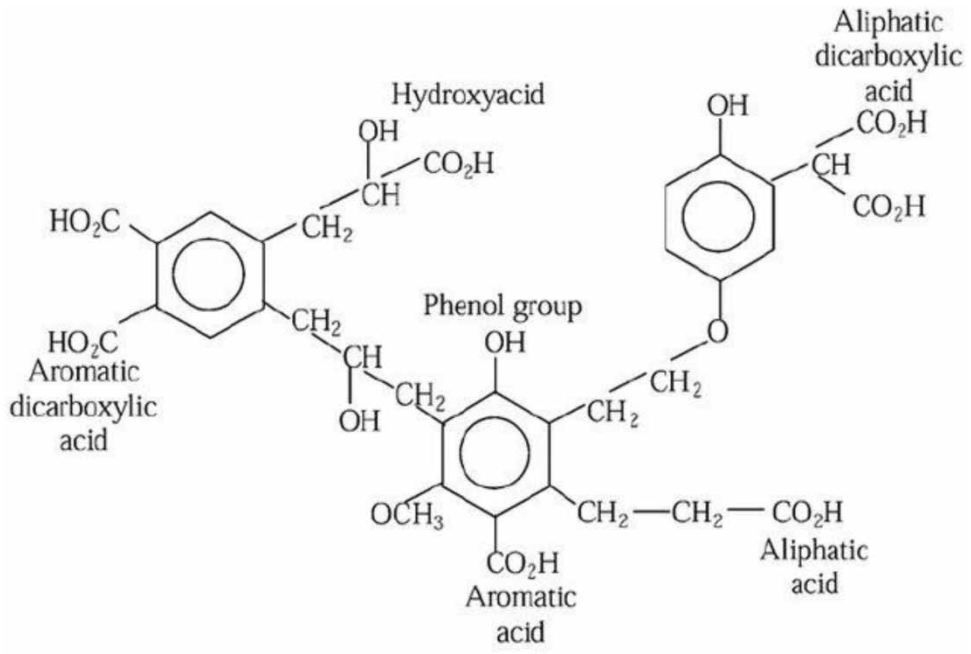

Figure 2 | Hypothetical molecular structure of humic acids (Duan & Gregory 2003).

The study of the impact of NOM on adsorption is very important since, in most cases, it reduces the adsorption capacity of activated carbon and its performance in removing CEC and other compounds (Domergue *et al.* 2022). This reduction in performance is due to its ability to compete for the adsorptive sites or pore blockage of the GAC (Ersan *et al.* 2016). Therefore, the presence of NOM in the solution can affect activated carbon's performance in removing an adsorbate of interest.

This research investigated the removal of carbendazim by adsorption on granular activated carbon through isotherms, adsorption kinetics, and RSSCT tests. The experiments were performed in two aqueous matrices, deionized water (DW) and DW solution with natural organic matter (DWNOM). Possible interference of NOM in the adsorption was investigated by comparing the results obtained in both matrices for each method tested (isotherms, kinetics, and RSSCT) and through statistical data analysis. CBZ was chosen because it has been one of the most widely used pesticides in Brazil in recent years. However, few studies on this compound have been carried out in the country, and no work until now has used the fixed-bed adsorption study approach. This research is believed to fill this knowledge gap.

2. METHODOLOGY

2.1. Isotherms

In the isotherm tests, variable concentrations of activated carbon (0.25; 0.50; 1.00; 2.00; and 5.00 g/L) were placed in Schott flasks containing 100 mL of water with a constant concentration of CBZ (5 mg/L). The flasks were placed in a water bath in a shaker equipment at 25 °C for 24 h. After this period, aliquots were removed from the flasks, separated on filters with size openings of 0.45 μm, and analyzed. The experiments were performed in triplicate in DW and DWNOM. All experiments were carried out in the pH range between 7 and 8.

The results were analyzed to determine which isotherm, Langmuir, Freundlich, Sips, or Redlich–Peterson best fitted the experimental data (Equations (1)–(4)). The parameters of the isotherms were determined using the nonlinear method with the Solver tool in Excel 2019. The coefficient of determination R^2 was also determined using this method and helped analyze the fit of the equations.

$$q_e = q_{max} \cdot \frac{b \cdot C_e}{1 + b \cdot C_e} \quad (1)$$

$$q_e = k_f \cdot C_e^{1/n} \quad (2)$$

$$q_e = \frac{q_{max} \cdot K_s \cdot C_e^{\frac{1}{ns}}}{1 + K_s \cdot C_e^{\frac{1}{ns}}} \quad (3)$$

$$q_e = \frac{k_{RP} \cdot C_e}{1 + a_{RP} \cdot C_e^{\beta}} \quad (4)$$

where C_e is the equilibrium concentration of CBZ in solution after adsorption (mg/L); q_e is the adsorbed amount of CBZ at equilibrium (mg/g); q_{max} is the maximum adsorption capacity (mg/g); b is the Langmuir equilibrium adsorption constant (L/mg); k_f is the Freundlich constant [(mg/g) (L/mg)$^{1/n}$]; $1/n$ is the Freundlich intensity parameter (–); K_s is the Sips equilibrium constant (L/mg)$^{1/ns}$; n_s is the Sips exponent (–); a_{RP} is the Redlich–Peterson equilibrium constant (L/mg)$^{\beta}$; k_{RP} is the constant incorporating the maximum sorption capacity and describing the adsorbent–adsorbate affinity (L/mg); and β is the exponent of the Redlich–Peterson isotherm (–).

2.2. Kinetics

The kinetics assays used a shaker with a constant temperature of 25 °C and pH between 7 and 8. Samples were collected in triplicate from Schott flasks containing 100 mL of solution with a constant concentration of 1 g/L GAC and 5 mg/L CBZ. The assays were performed in DW and DWNOM, with sample collection at regular times of 0, 10, 20, 30, 60, 120, 180, 240, 300, and 360 min.

The kinetic parameters were calculated using the nonlinear method with Excel's Solver function. The coefficients of determination R^2 were also determined using this method and helped analyze the fit of the equations. The pseudo-first-order, pseudo-second-order, and the intraparticle diffusion models (Equations (5) to (7), respectively) were tested. The intraparticle diffusion model considers that the linear coefficient C equals

zero if diffusion within the pore controls adsorption in the initial adsorption stages (Allen *et al.* 1989; Haro *et al.* 2017).

$$q_t = q_e(1 - e^{-k_1 t}) \tag{5}$$

$$q_t = \frac{q_e^2 k_2 t}{1 + q_e k_2 t} \tag{6}$$

$$q_t = k_{di} \cdot t^{0,5} + C \tag{7}$$

where q_t is the quantity of adsorbate removed per unit of adsorbent in time t (mg/g); q_e is the quantity of adsorbate adsorbed per unit of adsorbent at equilibrium (mg/g); k_1 is the first-order rate constant (min^{-1}); t is the contact time (min); k_2 is the second-order rate constant (g/mg min); k_{di} is the intraparticle diffusion constant (mg/g $min^{0.5}$).

2.3. Rapid small-scale column tests

Standards from a full-scale column were applied to determine the parameters used in the RSSCT column, as described in Table 1. The empty bed contact time (EBCT) for the reduced scale was calculated using the following equation.

Table 1 | RSSCT parameters and dimensions and the equivalent values for full scale

Parameter	Unit	Large scale	Small scale
GAC Granulometry	Mesh	8 × 30	60 × 80
Average diameter of the grains	mm	1.49	0.21
EBCT	min	5	0.72
Hydraulic loading rate	m^3/m^2·day	120.00	120.00
	m^3/m^2·h	5.00	5.00
Flow rate	mL/min	–	9.42
Apparent density	g/cm^3	0.65	0.65
GAC bed volume	cm^3	–	6.82
GAC bed height	cm	–	6.03

$$\mathrm{EBCT_{sc}} = \mathrm{EBCT_{lc}} \cdot \left(\frac{d_{p.sc}}{d_{p.lc}}\right)^{2-x} \tag{8}$$

where $\mathrm{EBCT_{sc}}$ is the EBCT in the small-scale column (min); $\mathrm{EBCT_{lc}}$ is the EBCT in the large column (min); $d_{p.sc}$ is the mean particle diameter of the small-scale column (mm); $d_{p.lc}$ is the mean particle diameter of the large-scale column (mm); x is the coefficient of dependence of particle size on intraparticle diffusivity, being 0 when diffusivity is constant (CD) and 1 when diffusivity is proportional (PD) to particle size.

Crittenden *et al.* (2012) suggest using the hydraulic loading rate (HLR) in adsorbent beds in the range 120–360 m^3/m^2·day (0.083 m^3/m^2·min), and the EBCT between 5 and 30 min. The design parameters considered an EBCT of 5 min and HLR of 120 m^3/m^2·day for a real-scale column. Applying this value in Equation (8), a time of 0.72 min was obtained for the reduced scale.

With the HLR and EBCT values, the reduced-scale column height could be calculated using the following equation.

$$H_{sc} = \mathrm{HLR_{sc}} \cdot \mathrm{EBCT_{sc}} \tag{9}$$

where H_{sc} is the small-scale bed height (cm); $\mathrm{HLR_{sc}}$ is the small-scale HLR, 120 m^3/m^2·day.

The flow rate of the reduced-scale adsorptive system was calculated using Equation (10). According to Summers *et al.* (2011), the flow rates for constant diffusivity (CD) and proportional diffusivity (PD) range from

50 to 150 mL/min and from 5 to 20 mL/min, respectively. The operating flow rate of the system, 9.42 mL/min, characterizing PD ($x = 1$ in Equation (8)).

$$Q_{sc} = \mathrm{HLR}_{sc} \cdot A_{sc} \tag{10}$$

where Q_{sc} is the flow rate (mL/min); and A_{sc} circular section area of the small-scale column (cm^2).

The internal diameter of the column was 1.20 cm. Table 1 details the parameters designed for the RSSCT and the values corresponding to a large-scale column.

From the results obtained in the RSSCT, it was possible to analyze the specific transfer rates (STR) and carbon utilization rates (CUR) through the following equations.

$$\mathrm{STR} = \frac{t_{\mathrm{breakthrough}}}{\mathrm{EBCT}_{ls} \cdot \rho_{GAC}} \tag{11}$$

$$\mathrm{CUR} = \frac{1}{\mathrm{STR}} \tag{12}$$

where STR is the specific transfer rate (cm^3/g); ρ_{GAC} is the density of bone GAC, equal to 0.65 g/cm^3; and CUR is the carbon use rate (g/L).

The reduction in adsorption capacity caused by organic matter is known as fouling (Corwin & Summers 2010). To evaluate this impact on the adsorption of CBZ on GAC, the Fouling Index equation (Equation (13)) was used to compare the breakthrough curves of the experiments performed on a reduced scale (Corwin & Summers 2010; Kennedy *et al.* 2017).

$$FI = SF^{\gamma} = \left(\frac{d_{p.lc}}{d_{p.sc}}\right)^{\gamma} \tag{13}$$

where FI is the fouling index; SF is the scaling factor; and γ is the fouling factor. As the comparison was performed between the reduced scales for both matrices, the ratio between the GAC diameters equals 1 ($d_{p.lc}/d_{p.sc} = 1$), as the same diameter range was used (60 × 80 mesh). The FI was calculated by nonlinear analysis using the Excel's Solver tool. Fixing ($d_{p.lc}/d_{p.sc}$) = 1, the value of γ was varied until a coefficient with the highest R^2 was found. Thus, the value of FI would be known, and the impact of fouling measured.

Due to the limitations of access and permanence in the laboratory at night, the analyses were not performed during this period. The experiments lasted 28 h because the saturation points had already been identified by the end of this period. To determine the breakthrough and saturation times, 5 and 90% of the initial CBZ concentration were considered. The experiments were performed in quadruplicate. All experiments were executed in the pH range between 7 and 8.

2.4. Activated carbon

Granular activated carbon (GAC) produced from bovine bones by Bonechar Company was used in the experiments. Grain and pore sizes were, respectively, 60 × 80 mesh and 0.48 to 14.93 nm. Because of its pore size, it is characterized as strictly microporous (Metcalf & Eddy 2014). Table 2 presents the specifications of activated carbon according to company information. However, the point of zero charge (PZC), total specific surface area (BET), and pore volume values were determined in the laboratory.

The PZC was calculated by the 11-point method by varying the pH from 2 to 12 using 1 N solutions of HCl and NaOH (Giacomni *et al.* 2017). Total specific surface area analysis and pore volume quantification followed the BJH/DH method in a Quantachrome NovaWin equipment using the temperature of 77.350 K, molar mass of Nitrogen of 28.013 kg/kmol, cross-section of 16.20 Â^2, net density of 0.808 g/cc and Boer's method of calculation (de Boer *et al.* 1966).

2.5. Solution with NOM

To prepare the solution containing NOM, sodium salt of humic acid from Sigma-Aldrich was dissolved in DW to obtain a concentration of 5 mg/L organic matter at pH 7. This concentration range has been previously used in experiments with RSSCT in studies with other pesticides (Plattner *et al.* 2018). Table 3 presents the specifications of humic acid according to company information.

Table 2 | Bone GAC specifications provided by the manufacturer[a]

Properties	Specifications
Carbon	9–11%
Acid-soluble ash	<3%
Insoluble ash	0.7
Tricalcium phosphate	70–76%
Calcium carbonate	7–9%
Calcium sulfate	0.1–0.2%
pH	8.5–9.5
Point of zero charge (PZC)	8.40
Total specific surface area (BET N^2)	57.78 m^2/g
Carbon surface area	50 m^2/g
Iron	<0.3%
Pore size	0.48–14.93 nm
Pore volume	0.0077 cm^3/g
Iodine number	93 mg/g
Humidity	<5%
Apparent density	0.60–0.70 g/cm^3
Hardness	>80
Aspect	Granulated and powdered solid
Smell	Odorless

[a]Except point of zero charge (PZC), BET specific surface area, and pore volume.

Table 3 | Humic acid specifications provided by Sigma-Aldrich

Appearance	Form: flakes; color: black, to, brown
Odor	Odorless
pH	No data available
Melting point/freezing point	Melting point/range: >300 °C
Initial boiling point and boiling range	>640 °C at ca. 1.013 hPa
Flammability (solid, gas)	The product is not flammable
Relative density	1.52 at 20 °C
Water solubility	369 g/L at 20 °C – regulation (EC)
Partition coefficient: n-octanol/water	log Pow: ca. −2.08 at 23 °C – bioaccumulation is not expected
Autoignition temperature	>400 °C at 1.013 hPa

The NOM was quantified by total organic carbon (TOC) analyses performed on a Shimadzu TOC-LCPH analyzer equipped with an automatic sample injector. The analyses were performed by thermal catalytic oxidation at 680 °C on platinum-coated alumina beads with a continuous supply of oxygen flow. The non-purgeable organic carbon (NPOC) method was used, and all procedures followed the standard equipment manual.

2.6. Carbendazim

Carbendazim was purchased from Sigma-Aldrich, with a purity of 97%. The CBZ was initially dissolved in an acidic medium (pH between 2.7 and 3.0) with 1 N H_2SO_4 to accelerate the compound's dissolution. Afterwards, the pH of the solution was raised to a range between 7 and 8 by adding 1 N NaOH. The experiments were carried out in this pH range. For the analysis of CBZ, a Shimadzu LC20A High-Performance Liquid Chromatograph (CLAE – HPLC) equipped with a diode array detector (DAD, SPD-20AV) and autosampler (SIL-20A) was used. The concentration of CBZ used in the experiments was 5 mg/L, dissolved in DW and water containing

organic matter (DWNOM). This concentration of CBZ was used due to better monitoring of the adsorptive process and had already been used in similar experiments with higher concentrations (Li *et al.* 2022).

2.7. Statistical treatment

One of the most widely used methods is Kendall's (Kendall 1938), which can be represented by graphical displays or mathematical models, showing a trend or how the data are affected by other independent variables (Davis & Chen 2007). Kendall's regression coefficient indicates the extent to which the response variable can be approximated by a strictly increasing function of the predictor variables (Liebscher 2021).

The Kruskal–Wallis method is a non-parametric statistical test that assesses whether two or more samples are drawn from the same distribution (Guo *et al.* 2013). This method is used when the experimental data do not have a normal distribution and is especially suitable in cases where the data size is small. The Kruskal–Wallis method is generally used when two or more independent groups (of equal size or not) with a quantitative response variable are analyzed (Hollander & Wolfe 1973).

Statistical analyses were performed to verify the interference of DWNOM in the adsorptive process compared to DW. The analysis included correlation, determination, and significance tests using R software version 4.0.4. Kendall's method was applied to identify the correlation between the applied GAC dosages and the remaining CBZ concentrations. For the significance tests in the RSSCTs, the Kruskal–Wallis method ($p < 0.05$) was used to compare the results for the different contact times in the DW and DWNOM matrices.

3. RESULTS AND DISCUSSION

3.1. pH test

Before the tests with NOM, a study was conducted to identify the pH at which the activated carbon would perform better. This was done using 5 mg/L of CBZ in DW and a concentration of 1 g/L of bone GAC at pHs of 2, 4, 6, 8, and 10. To check if there was a significant difference between the pHs, the *t*-Student test was applied. An analysis using the Shapiro–Wilk test found that the results of this approach had a normal distribution. The test indicated that the performance of the GAC in CBZ removal at pH 8 did not differ significantly from that of the acidic medium. Therefore, all experiments were performed in the pH range between 7 and 8.

3.2. Activated carbon characterization

The considerations in this topic refer to Table 2, which shows the GAC characterization. The presence of calcium carbonate, calcium sulfate, and tricalcium phosphate in the GAC may be a factor favoring the adsorption of organic matter and consequently reducing the adsorption of CBZ. Bivalent cations such as calcium can interact with organic matter, increasing its adsorption capacity by forming complexes (Summers *et al.* 2011).

The density value is within the usual range for activated carbons (0.35–0.65 g/cm^3) (Summers *et al.* 2011). The specific surface area value, 57.78 m^2/g is lower than that recommended by AWWA (2005) for adsorption by granular activated carbon in water supply systems (650–1,000 m^2/g). This is also observed for the iodine number, whose recommended range is 600–1,100 mg/g (Metcalf & Eddy 2014). Although these parameters are indicators of the adsorptive capacity of activated carbon, the performance of GAC is generally best evaluated through isotherm and column experiments at the laboratory scale or pilot scale. This is particularly true for the removal of CEC in drinking water (Summers *et al.* 2011).

The experiments occurred in pH between 7 and 8, below the PZC value of 8.4 (Table 2). This pH value for PZC was also found in other studies for activated carbon (Miyittah *et al.* 2016). Thus, the carbon surface showed slightly cationic characteristics, more prone to adsorb substances with anionic components, such as organic matter.

The anionic form of CBZ predominated in the assays, considering its pKa of 4.53 $\pm$ 0.07 and pH of the medium between 7 and 8 (Mazellier *et al.* 2002). Thus, considering the configuration of the surface molecules of GAC and CBZ, there might be an electrostatic attraction between the compounds, favoring adsorption.

Crittenden *et al.* (2012) stated that molecules with a molar mass of around 10^2 g/mol have a particle size of less than 0.01 nm. Considering that the molar mass of CBZ is 191.19 g/mol and the porosity of GAC varies between 0.48 and 14.93 nm, it can be concluded that the CBZ molecules could access the GAC pores.

Supplementary material shows a GAC picture generated with scanning electron microscopy, highlighting the grains and the GAC pores.

3.3. Isotherms

The results of the isotherm tests are presented in Figure 3 and Table 4. All the tested models fitted well to the adsorption of CBZ in both DW and DWNOM. In DW, the Freundlich and Sips isotherms had R^2 of 0.98, slightly higher than Langmuir (0.97) and Redlich–Peterson (0.93). For DW with organic matter, all models had the same R^2 (0.91). Figure 3 shows that the presence of organic matter influenced the equilibrium concentrations for each mass of GAC used.

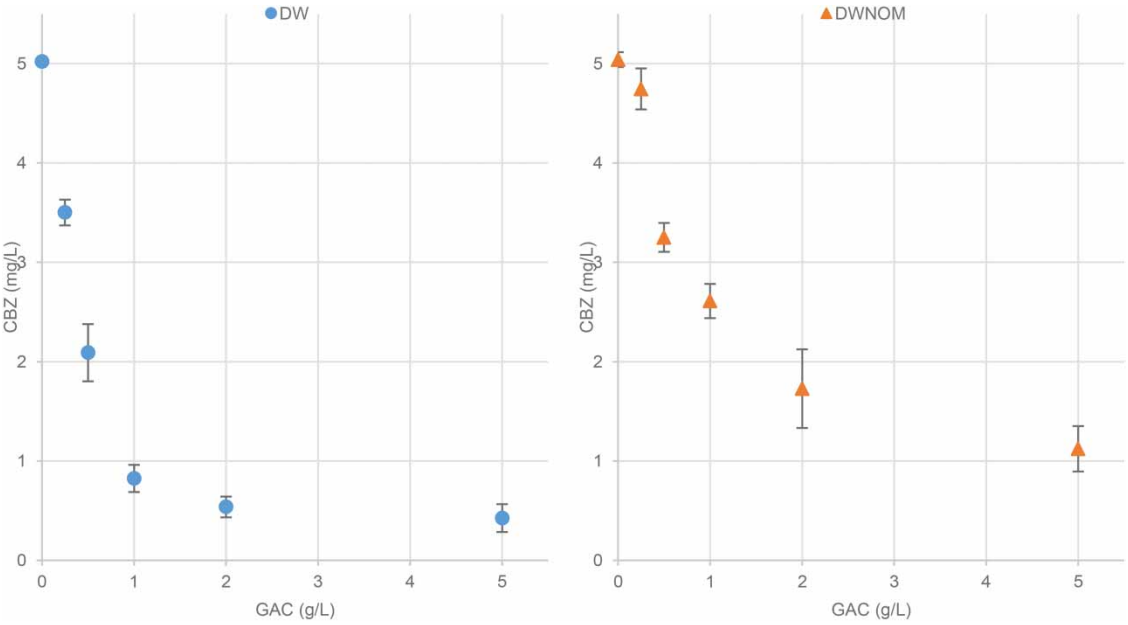

Figure 3 | Results of the tests for the DW and DWNOM experiments (means ± standard deviation, $n = 3$).

Table 4 | Parameter values and determination coefficients for the Freundlich, Langmuir, Sips, and Redlich–Peterson isotherms

Model	Parameter	DW	DWNOM
Freundlich	K_f (mg/g)(L/mg)$^{1/n}$	60.49	17.09
	$1/n$	0.67	1.09
	R^2	0.98	0.91
Langmuir	$q_{máx}$ (mg/g)	159.10	564,423.77
	b (L/mg)	0.49	0.00
	R^2	0.97	0.91
Sips	$q_{máx}$ (mg/g)	159.10	869,460.22
	K_s (L/mg)$^{1/ns}$	0.49	2.18×10^{-5}
	Ns	1.00	1.00
	R^2	0.98	0.91
Redlich–Peterson	a_{RP} (L/mg)$^{\beta}$	0.00	0.00
	k_{RP} (L/mg)	32.72	19.24
	β	0.00	0.00
	R^2	0.93	0.91

The Redlich–Peterson β value must be greater than 0 ($0 < \beta \leq 1$) (Dehghani Karri & Lima 2021). As the fitted model resulted in $\beta = 0$, it may be that this model does not adequately fit the adsorption of CBZ on GAC in DWNOM. The Langmuir's and Sips' q_{max} values were very high for DWNOM. These values may indicate that these isotherms are not the most adequate to represent the adsorption of CBZ on GAC for the analyzed conditions (Almeida *et al.* 2023). Considering these particularities and the R^2 values, it was considered that the Freundlich model best described the adsorption of carbendazim on both matrices.

The Freundlich isotherm indicates the possibility of heterogeneous multilayer formation during adsorption (Piccin *et al.* 2017; Haro *et al.* 2021). Thus, the adsorption of CBZ may also present this characteristic, with the formation of multilayers in both tested matrices.

For comparison purposes, the Freundlich isotherm was used to represent the adsorption of CBZ on DW and DWNOM (Equations (14) and (15), respectively). Figure 4 shows the graphs obtained from the equations.

$$q_e = 60.49 \times C_e^{0.67} \tag{14}$$

$$q_e = 17.09 \times C_e^{1.09} \tag{15}$$

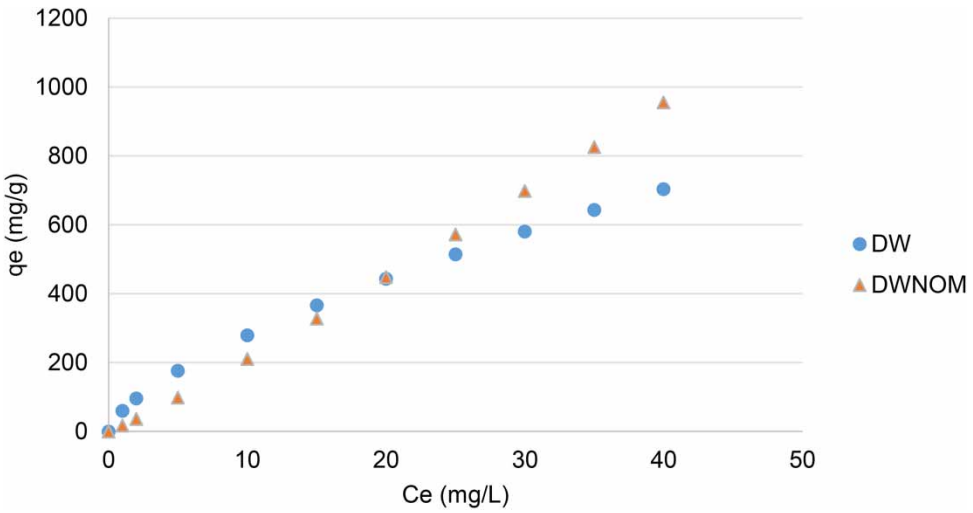

Figure 4 | Freundlich isotherms for the adsorption of CBZ on DW and DWNOM.

Figure 4 indicates that, for the same equilibrium concentrations (C_e), the amount of CBZ adsorbed per gram of GAC (q_e) is higher in DW than with the presence of organic matter up to a specific equilibrium concentration (20 mg/L). At this point, the Freundlich curve for CBZ in DWNOM crosses that of DW, indicating a change in the adsorption dynamics of CBZ in this medium. This crossing in q_e and C_e was also observed in kinetics and RSSCT. Although there was interference of NOM on adsorption, the removal of CBZ was satisfactory in both matrices. Thus, bovine bone GAC was efficient in removing CBZ in DW and DWNOM.

There was a 72% reduction in the Freundlich constant (K_f) of the isotherm with DWNOM compared to DW. The reduction in K_f is interpreted as direct competition and pore blocking of the activated carbon (Pelekani & Snoeyink 1999). It was observed that the Freundlich intensity parameter (1/n) for adsorption on DW was less than unity, indicating that the adsorption of CBZ on bone GAC was a favorable process (Anfar *et al.* 2020). This was also observed using other adsorbents (Paszko 2006; Li *et al.* 2011; Jin *et al.* 2013; Rizzi *et al.* 2020; Wang *et al.* 2020). For DWNOM, the $1/n$ value slightly above one (1.09) suggested that organic matter impacted the adsorptive process of CBZ in GAC. Changes in the value of 'n' are interpreted as changes in the distribution of energy sites of the adsorbent (Pelekani & Snoeyink 1999), which means that the presence of humic acid (NOM) might have affected the distribution of the adsorptive sites of bovine bone GAC. This resulted in a change in the shape of the Freundlich isotherm curve.

Table 5 presents the results of the correlation tests applying the Kendall method, analyzing the variables 'GAC dosages' and 'CBZ concentrations' at equilibrium for each matrix.

Table 5 | Result of applying the Kendall method to the isotherm test

Matrix	Correlation coefficient (τ)	Determination coefficient (τ^2)
DW	−1.00	1.00
DWNOM	−0.60	0.36

The values indicated a strong correlation between the amount of GAC and the final concentration of CBZ in DW. The adsorption of CBZ in DW was inversely proportional to the dosage of GAC, i.e., the greater the amount of adsorbent used, the lower the concentration of CBZ remaining in the solution. For DWNOM, the value of τ^2 was low. Although the inverse relationship between the adsorbate and the adsorbent remained, it was weaker than in DW.

3.4. Kinetics

The results of the experiments investigating the adsorption kinetics are shown in Figure 5 and Table 6. For both matrices, the pseudo-second-order kinetics best fitted the adsorption process ($R^2 = 0.98$ in DW and $R^2 = 0.99$ in DWNOM). The pseudo-first-order kinetics also fitted the adsorption of CBZ on GAC in both DW and DWNOM, with higher R^2 obtained in the medium with organic matter. Intraparticle diffusion was not a determinant in the initial steps of the adsorption process in both matrices. A good fit was achieved in the adsorption of CBZ on GAC for DWNOM ($R^2 = 0.93$).

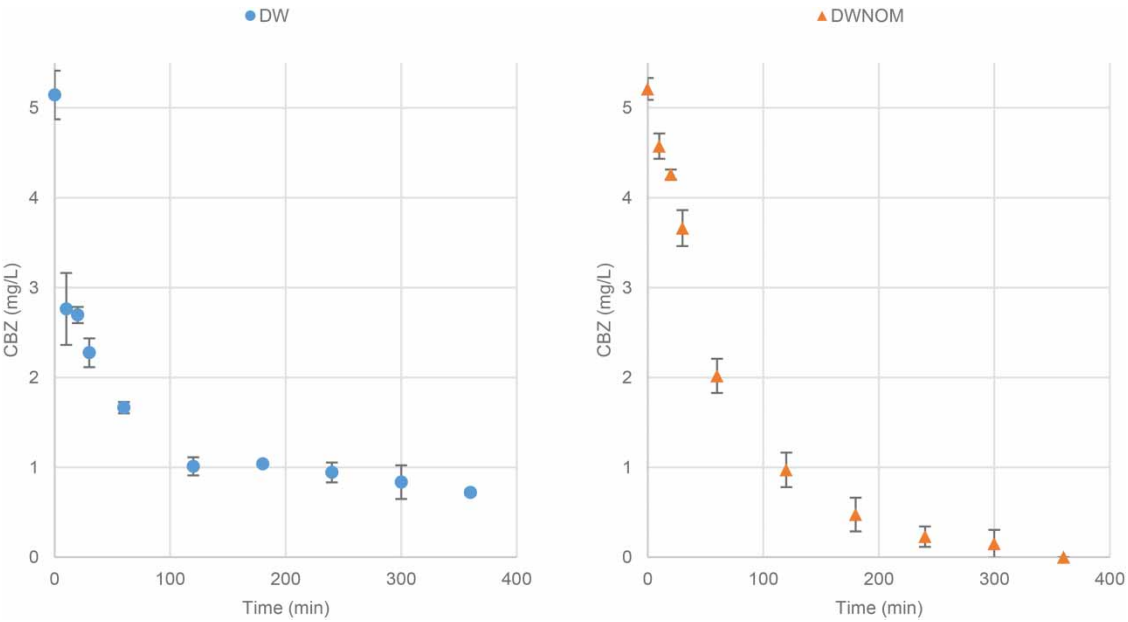

Figure 5 | Results of the kinetics tests for the experiments in deionized water (DW) and deionized water with organic matter (DWNOM) (means ± standard deviation, $n = 3$).

Table 6 | Parameter values and coefficients of determination for the pseudo-first-order and pseudo-second-order models and intraparticle diffusion

Model	Parameter	CBZ in DW	CBZ in DWNOM
Pseudo-first-order	K_1 (t^{-1})	0.049	0.019
	q_e (mgCBZ/gGAC)	4.157	5.902
	R^2	0.94	0.99
Pseudo-second-order	K_2 (t^{-1})	0.017	0.003
	q_e (mgCBZ/gGAC)	4.462	6.987
	R^2	0.98	0.99
Intraparticle diffusion	K_{dt}	0.189	0.330
	C	1.419	0.615
	R^2	0.79	0.93

The pseudo-second-order kinetic models that best-fitted carbendazim's adsorption in DW and DWNOM are shown in Equations (16) and (17), respectively. Figure 6 shows the relations between q_t and t from these

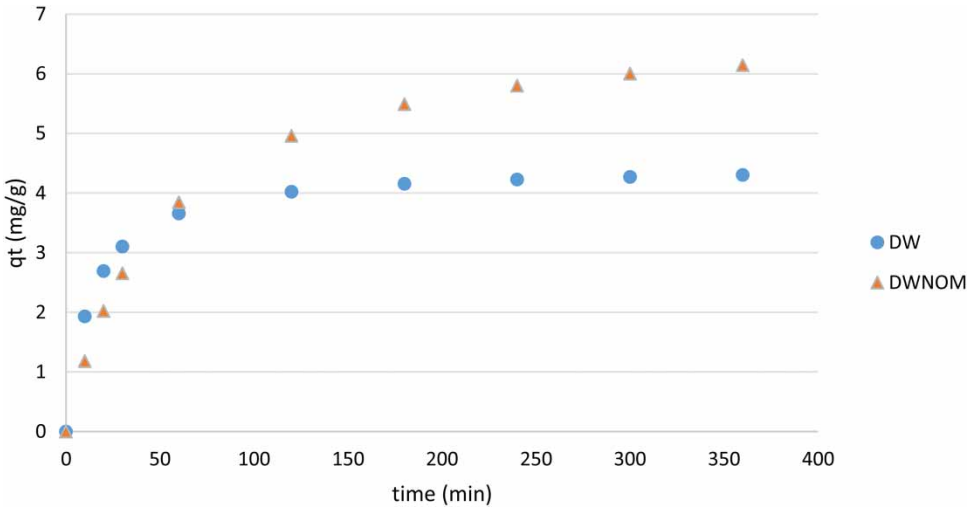

Figure 6 | Adsorption kinetics of CBZ in deionized water (DW) and deionized water with organic matter (DWNOM). q_t is the amount of adsorbate removed per unit of adsorbent in time t, in mg/g.

equations.

$$q_t = \frac{0.34 \times t}{1 + 0.08 \times t} \tag{16}$$

$$q_t = \frac{0.14 \times t}{1 + 0.02 \times t} \tag{17}$$

The results showed that the adsorption capacity of CBZ by GAC was initially higher in DW. However, after approximately 60 min, the adsorption capacity of CBZ by GAC in DWNOM increased and exceeded the amount of CBZ adsorbed in DW for the same experimental times. The same occurred in the isotherm experiments, as illustrated in Figure 4. The explanation for this change in adsorption dynamics is uncertain. One hypothesis is that, because of their larger size and molecular weight, the organic matter particles may have pulled the CBZ molecules together to the GAC surface, thus increasing the concentration removed from the fungicide. Zhu *et al.* (2023) showed that the presence of DOM enhanced the adsorption of heavy metals onto GAC at 5 mg/L DOM concentrations. Thus, another hypothesis is that NOM may have improved GAC's ability to adsorb the fungicide.

The pseudo-second-order equation was also the best fit for the adsorption of CBZ of the herbicide Linuron on activated carbon (Hgeig *et al.* 2019). Similarly, the adsorption of atenolol on GAC was best represented by pseudo-second-order kinetics (Haro *et al.* 2017). Cao *et al.* (2011) found that the pseudo-second-order equation represented better the adsorption of p,p′- and o,p′-dichloro-diphenyl-trichloroethane (DDT) on sediments. The same was identified for the adsorption of the insecticide fenitrothion and the herbicide trifluralin on organo-zeolites and activated carbon (Lule & Atalay 2014) and for the adsorption of cobalt (II) and nickel (II) from hydrometallurgical effluent by modified clinoptilolite (Kaduba & Banza 2020).

About GAC intraparticle diffusion, it was possible to infer that it was stronger in the adsorption of CBZ in DWNOM than DW. This can be attributed to the organic matter, which altered the adsorption dynamics of the fungicide and generated a deviation from the origin of the graph (Figure 7). The moderate coefficient of determination (0.79) showed that intraparticle diffusion was not a step determining the speed of adsorption of CBZ in GAC in DW.

Equation (18) represents the model of the intraparticle diffusion in DWNOM using the data shown in Table 6. Figure 7 shows the relation between q_t and t.

$$Q_t = 0.33 \cdot t^{0.5} + 0.62 \tag{18}$$

Two distinct stages of the adsorptive process of CBZ on GAC can be observed. The first step (Phase I) was related to the adsorption on the adsorbent's external surface and represented the linear boundary layer effect.

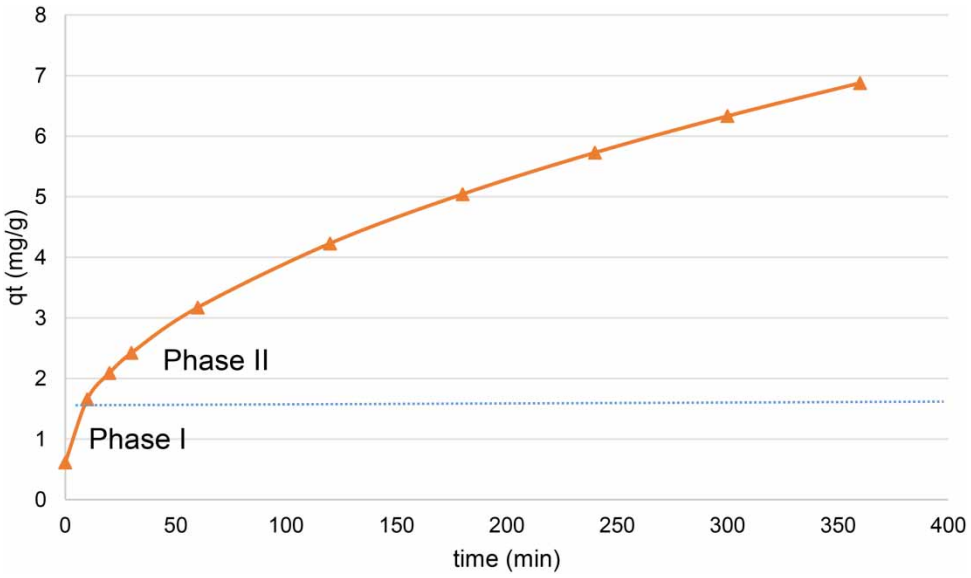

Figure 7 | Figure illustrating the intraparticle diffusion in the adsorption of CBZ on GAC in DWNOM, from Equation (18). q_t is the amount of adsorbate removed per unit of the adsorbent in time t, mg/g.

The second region (Phase II) represented intraparticle diffusion. The phase representing the equilibrium in adsorption, where the adsorbed amount is constant (Phase III), was not observed (Ruiz *et al.* 2010; Haro *et al.* 2017; Del Vecchio *et al.* 2019). Thus, for the adsorption of CBZ, the phase related to intraparticle diffusion exerted more influence on the adsorptive process than the boundary layer effect. However, this may have occurred because the equilibrium was not reached.

The adsorption study of CBZ on activated carbon by Hgeig *et al.* (2019) showed a high coefficient of determination when fitting the intraparticle diffusion equation. As in the present study, the equation did not start from the origin in the early stages of the adsorptive process. The authors concluded that adsorption on the surface of the GAC had the most significant influence at the beginning of the experiments, with intraparticle diffusion playing a limiting role in adsorption. In the present study, it was possible that the deviation from the origin occurred due to the difference in mass transfer rate between the initial and final stages of adsorption (Ahmed & Theydan 2012; Del Vecchio *et al.* 2019).

Larger GAC particles result in slower adsorption kinetics since this is inversely proportional to the square of the GAC particle diameter (Kennedy *et al.* 2015). According to the pore size and volume shown in Table 2, the GAC used in the experiments was strictly microporous. Thus, the change in adsorption dynamics is believed to be due exclusively to the organic matter, as the pores of the carbon did not act as a limiting factor on the adsorption kinetics of CBZ.

Table 7 shows Kendall's statistical test results in analyzing the variables 'Time' and 'CBZ concentrations' for each matrix.

Table 7 | Result of application of the Kendall test relating the variables time and CBZ concentrations in the kinetics assays

Matrix	Correlation coefficient (τ)	Determination coefficient (τ^2)
DW	−0.75	0.56
DWNOM	−0.87	0.76

A moderate negative correlation between time and CBZ concentrations can be observed. In both matrices, the longer the contact time, the lower the concentration of CBZ remaining in the solution. This is consistent with previous studies that used 2–24 h equilibrium times for CBZ adsorption (Paszko 2006; Li *et al.* 2011; Jin *et al.* 2013; Rizzi *et al.* 2020; Wang *et al.* 2020). Although contact time was the only variable factor (medium temperature, GAC concentration, pH, and CBZ concentration remained constant), a low τ^2 value was observed for DW.

Figure 5 shows that there was no increase in the adsorption of CBZ in DW on GAC after a certain time, which might explain the low τ^2 value.

3.5. Rapid small-scale column tests

Figures 8 and 9 and Table 8 show the Rapid Small-Scale Columns Tests (RSSCT) results. The breakthrough time (considered as $0.05C_0$) was longer for the GAC column in the configuration of CBZ with DW. The column saturation time for CBZ adsorption ($0.90C_0$) was higher with the presence of organic matter.

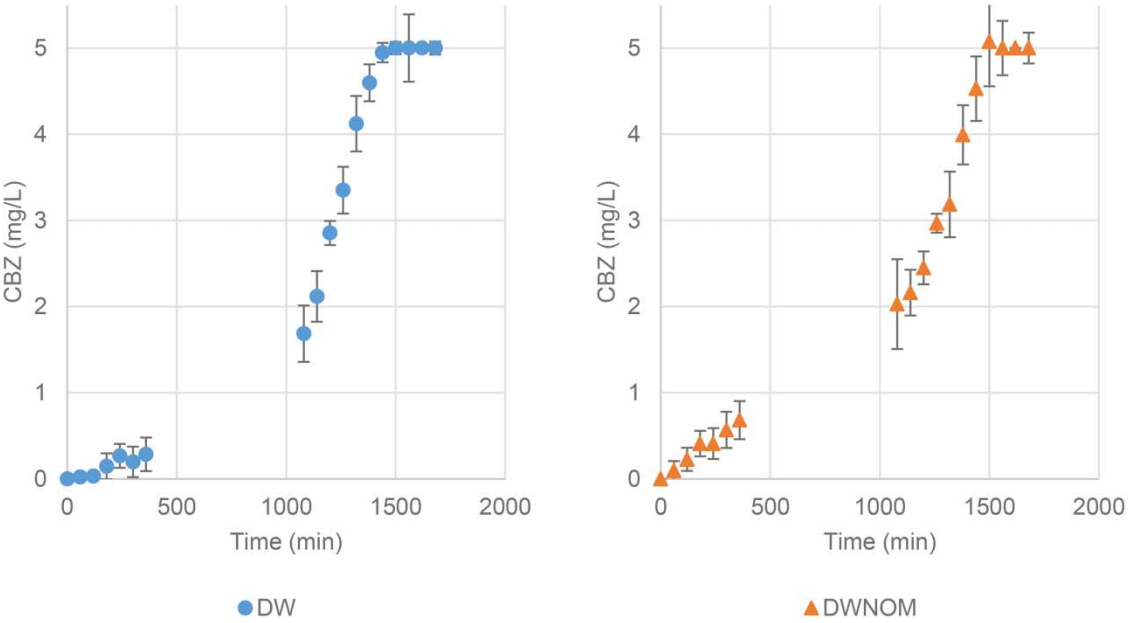

Figure 8 | Results of the small-scale column rapid tests (RSSCT) for deionized water (DW) and deionized water with organic matter (DWNOM) experiments (mean ± standard deviation, $n = 4$).

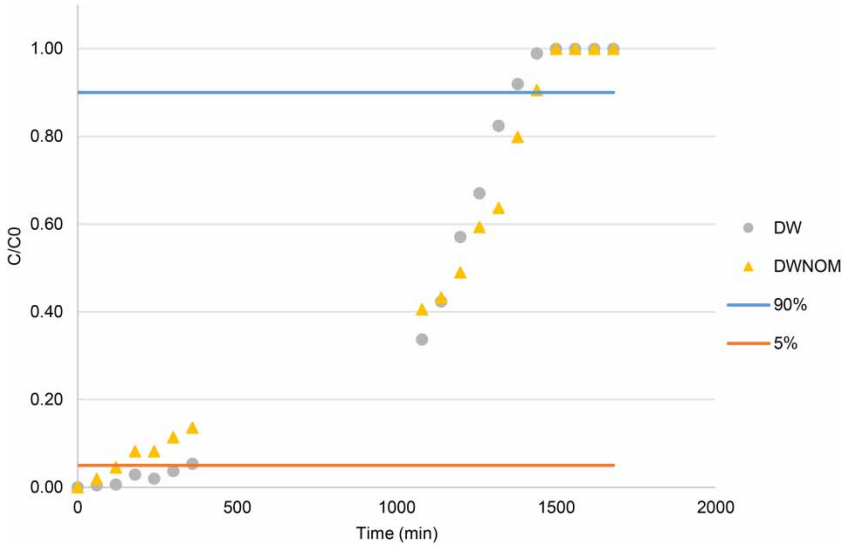

Figure 9 | CBZ breakthrough curves obtained from the RSSCT for the experiments in deionized water (DW) and deionized water with organic matter (DWNOM).

Figure 10 shows the breakthrough curve in the RSSCT test with the affluent containing only organic matter. NOM was present in the effluent of the GAC column early in the column operation. This was also observed in tests performed by Mavaieie & Benetti (2021).

Table 8 | Relationship between final (C) and initial (C_0) concentrations for each time collected in the RSSCT

T (min)	CBZ in DW C/C_0	CBZ in DWNOM C/C_0
0	0.00	0.00
60	0.00	0.02
120	0.01	0.05
180	0.03	0.08
240	0.02	0.08
300	0.04	0.11
360	0.05	0.14
1,080	0.34	0.41
1,140	0.42	0.43
1,200	0.57	0.49
1,260	0.67	0.59
1,320	0.82	0.64
1,380	0.92	0.80
1,440	0.99	0.91
1,500	1.00	1.00
1,560	1.00	1.00
1,620	1.00	1.00
1,680	1.00	1.00

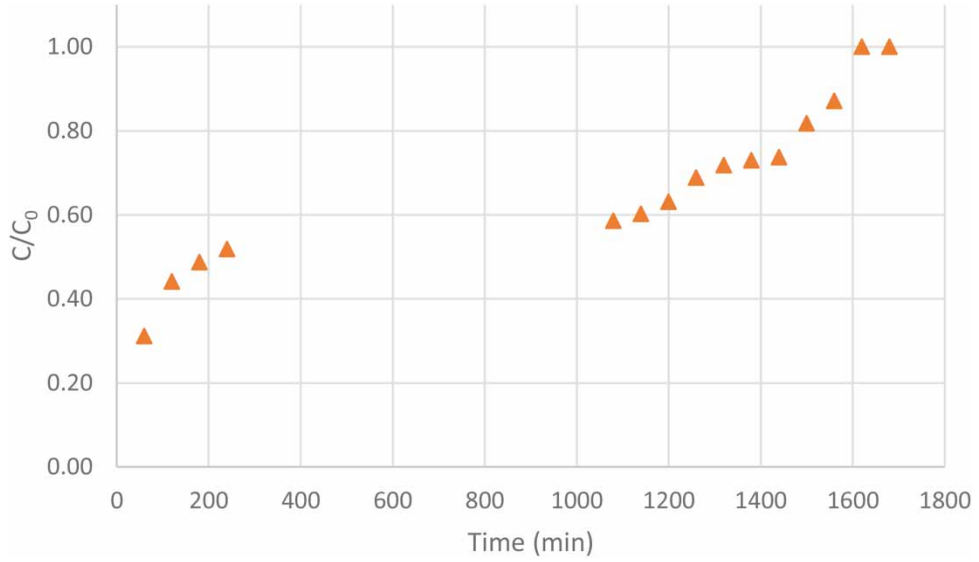

Figure 10 | Breakthrough curve in RSSCT test with affluent containing only natural organic matter (NOM).

Table 9 presents the breakthrough and saturation times of the CBZ in DW and DWNOM. The Specific Transfer Rate (STR) and Carbon Utilization Rate (CUR) values calculated with Equations (11) and (12) are also presented. The results for DW and DWNOM were distinct, with organic matter influencing CBZ adsorption in the RSSCT assays.

STR and CUR are parameters used to analyze the performance of GAC in contaminant removal. The higher the STR values and, consequently, the lower the CUR values, the higher the efficiency of GAC and the more economical its application in water treatment (Kennedy *et al.* 2015; Kempisty *et al.* 2022). The highest efficiency of GAC was in the configuration of CBZ in DW, in which there was no competition for the adsorption sites.

Table 9 | Breakthrough times, saturation times, and values of specific transfer and carbon utilization rates in DW and DWNOM

Tests	Breakthrough time (min)	Saturation time (min)	STR (cm^3/g)	CUR (g/L)
DW	360	1,440	110.8	9.0
DWNOM	120	1,500	36.9	27.1

DW, deionized water; DWNOM, deionized water with organic matter.

Specific adsorption studies of CBZ using RSSCT were not found in the literature. However, other substances have already been studied using this methodology. Coelho & Rozário (2019) reported the removal of the herbicide 2,4-D. They found the breaking point in ultrapure water at 1,349 min, higher than the time measured in the CBZ tests and, therefore, lower CUR. The authors used an initial 2,4-D concentration of 7 μg/L, EBCT of 0.72 min, a 6.5 mL/min flow rate, and a GAC bed height of 6 cm for the reduced scale. The authors considered, as a breaking point, the maximum 2,4-D concentration allowed by Brazilian legislation.

In another study, Voltan *et al.* (2016) evaluated the removal of the herbicides diuron and hexazinone in GAC, having obtained a CUR of 10.7 mg/L. In this case, EBCT values ranged from 0.0251 to 0.0548 min, with a flow rate of 1.85 mL/min and a GAC bed height of 25 cm. The maximum diuron and hexazinone concentrations allowed by Brazilian legislation were considered as the breaking point.

Comparing the results calculated for CUR, it is observed that the GAC showed lower performance in CBZ removal compared to the cited studies. Different operational conditions, such as GAC bed height, flow rates, EBCT, and initial concentrations of adsorbates, may have influenced the results.

As for the relationship between the experiments performed in RSSCT and the FI (Equation (13)), it was observed that the fouling factor (ϒ) had no impact on the adsorption of CBZ, regardless of the values tested in the application of the method. The coefficient of determination (R^2) obtained was equal to 0.98 for all values of ϒ modeled by the Solver. The breakthrough curve of CBZ in DW in GAC multiplied by the values of each time with the Fouling Factor (SF) resulted in a breakthrough curve identical to the one obtained with the adsorption of the compound in DW without the addition of SF. Also, the breakthrough curve for the RSSCT containing CBZ and NOM showed a coefficient of determination of 0.98 relative to the adsorption curve of CBZ dissolved in DW. This indicates that the addition of a coefficient was not necessary. Thus, for the conditions analyzed, the impact of fouling on the adsorption dynamics of CBZ in GAC was considered negligible.

Table 10 shows the statistical test results applying the Kendall method to the data measured in the RSSCT assays, analyzing the variables 'Time' and 'CBZ concentrations' for each matrix. The values showed a moderate positive correlation between time and CBZ concentrations, indicating that the concentration of CBZ in the column effluent increases with operating time.

Table 10 | Result of applying the Kendall method to the RSSCT

Matrix	Correlation coefficient (τ)	Determination coefficient (τ^2)
DW	0.80	0.64
DWNOM	0.90	0.81

Table 11 shows the results of the Kruskal–Wallis significance tests performed comparing the results measured in the two aqueous matrices for each sampling time.

Table 11 shows that, only at the time of 120 min, there was a significant difference ($p < 0.05$) between CBZ adsorption in DW and DWNOM. It is noted that 120 min was the breakthrough point in DWNOM, suggesting a change in the CBZ adsorption dynamics in this medium. On the other hand, the breakthrough and saturation times for the experiment in DW (360 and 1,440 min, respectively) and the saturation point for DWNOM (1,500 min) had no statistically significant differences. This trend was consistent with the fouling test results, which indicated that the impact of organic matter was negligible in the small-scale fixed bed.

Table 11 | Analysis of the difference between CBZ concentrations dissolved in deionized water (DW) and with natural organic matter (DWNOM) for the same dosage of GAC ($p < 0.05$)

Time	*p*-value
0	–
60	0.54
120	0.04
180	0.08
240	0.25
300	0.08
360	0.08
1,080	0.81
1,140	0.62
1,200	0.18
1,260	0.08
1,320	0.18
1,380	0.18
1,440	0.46
1,500	0.65
1,560	0.12
1,620	0.48
1,680	0.26

Although the interference of organic matter on CBZ adsorption was detected through the distinct breakthrough and saturation times, STR and CUR, the final concentrations analyzed were statistically similar. Thus, it can be considered that the column that received CBZ in DW had a better performance in terms of STR and CUR compared to DWNOM, since it had a longer time to reach the breaking point but a similar saturation time.

3.6. General considerations on the impact of organic matter on CBZ adsorption

After performing the isotherms and kinetics tests, it was found that the presence of NOM in the form of humic acid changed the adsorption parameters. This result was mainly due to the physicochemical properties and interactions between the organic matter, the fungicide, and the activated carbon. A possible explanation for this effect was the adsorption of larger molecules of NOM on the outer surface of the GAC, blocking the pore entrance and reducing the number of accessible adsorptive sites (Domergue *et al.* 2022). This process might have decreased CBZ adsorption over time (Moussavi *et al.* 2013). This interference was most evident in the isotherm experiments.

Because they have different molecular sizes, the competition for the sites observed in the experiments was mainly due to the pore size distribution of the GAC since the organic matter can occupy the macropores and mesopores, preventing the access of CBZ to the micropores of the adsorbent. Thus, the GAC's pore distribution controlled the competition mechanism (Pelekani & Snoeyink 1999). Microcontaminants in drinking water are usually present in concentrations three to six orders of magnitude smaller than NOM. This implies a reduced adsorption capacity in the presence of NOM (Domergue *et al.* 2022)

Another interference factor in the adsorption process is the electrostatic interactions between the organic matter and the activated carbon, which can favor its adsorption. The organic matter in the form of humic acid is negatively charged in the pH range in which the experiments were performed. Thus, it can compete with the anions of the CBZ molecule for the activated carbon pores, which are positively charged (Moussavi *et al.* 2013). As already shown in the characterization of the activated carbon, the presence of bivalent cations of the GAC may have favored these electrostatic interactions and enabled the adsorption of organic matter by this process.

It is possible that NOM could have improved the efficiency of GAC in removing CBZ. This is possible because some organic compounds change their fate in the presence of humic substances (Carter & Suffet 1982).

Guillossou *et al.* (2020) identified that a pre-equilibrium of 24 h between organic micropollutants (OMP) and dissolved organic matter (DOM) improved their removal onto powdered activated carbon. Their results showed the formation of DOM-OMPs complexes in solution, which increased the overall removal of OMPs, especially at short contact times. Similarly, Zhu *et al.* (2023) showed that the presence of DOM enhanced the adsorption of heavy metals onto GAC at 5 mg/L DOM concentrations. Our study did not include a pre-equilibrium period between CBZ and NOM. However, this may be a possibility for the increase in the adsorptive capacity of CBZ on GAC in DWNOM, especially in the RSSCT, where there was a contact time of more than 24 h between CBZ and NOM in the reservoir that fed the GAC column.

CEC adsorption is mainly influenced by kinetic factors, which are affected by the interaction between NOM and trace molecules. As a result, NOM impacts the removal of target contaminants (Domergue *et al.* 2022). Based on the collected data from the experiments, and comparison with previous studies, it was observed that organic matter interacted with the adsorptive sites of bovine bone GAC, altering the adsorption dynamics of CBZ, especially in the batch experiments.

The fixed-bed experiments showed different results, reflected by breakthrough and saturation times, STR and CUR values. However, the data generated were statistically similar, and there was no evidence of compromise in the efficiency of the activated carbon. The results of the kinetics and RSSCT tests may indicate an improvement in the adsorption of CBZ due to the presence of NOM. Furthermore, the fouling analysis showed that the effect of organic matter was negligible for small-scale fixed beds.

4. CONCLUSIONS

The isotherms, kinetics, and RSSCT experiments showed that activated carbon removed CBZ in both aqueous matrices. In the adsorption experiments for CBZ dissolved in deionized water with organic matter (DWNOM), the four isotherm models tested had equal determination coefficients (0.91). For CBZ dissolved in DW, the Freundlich and Sips models had the highest determination coefficients (0.98). However, the Langmuir and Redlich–Peterson isotherms also fit the CBZ adsorption with coefficients of 0.97 and 0.93, respectively. The K_f and $1/n$ parameters of the Freundlich isotherm, which simultaneously fitted the adsorption of CBZ dissolved in DW and DWNOM, varied according to the matrix, evidencing the interference in adsorption by NOM.

For the tests with kinetics, it was found that the pseudo-second-order model fitted best the adsorption of CBZ on GAC in both matrices. The results showed that in the initial stages of adsorption, the adsorptive capacity was higher in the configuration in which CBZ was dissolved in DW. However, the adsorption capacity of CBZ dissolved in DWNOM increased during the same experimental times of CBZ in DW. The same occurred in RSSCT. Thus, the data showed that the presence of organic matter, under the conditions analyzed, improved the efficiency of GAC in adsorbing CBZ in kinetics and RSSCT tests. Intraparticle diffusion was more intense in DWNOM than in DW, with adsorption on the outer surface of the GAC exerting a more significant influence. In both matrices, the pseudo-first-order model also adjusted the data well.

The RSSCT results showed that organic matter reduced the time required to reach a breakthrough compared to the pure aqueous matrix, evidencing a significant difference between the results. The concentrations of CBZ effluent from the GAC bed were different at all collection times analyzed, reflecting different saturation times, STR, and CUR. However, there was no statistically significant difference in the breakthrough curve for most of the data. The fouling study indicated that NOM did not significantly impact the CBZ breakthrough curve. Thus, even with differences between the fixed-bed adsorption curves, the results were considered similar.

The results indicated that the presence of organic matter impacted the adsorption of CBZ, changing the dynamics in the isotherm and kinetics tests. This influence was evidenced in the different parameters obtained for all the methods tested. For the fixed-bed experiment, most of the results were statistically similar, although distinct data were observed. Despite having an impact on the adsorption of the fungicide, NOM may have improved the ability to remove CBZ, especially in the kinetics and RSSCT tests. This may have been due to a possible interaction between CBZ and humic acid.

Based on the isotherms, kinetics, and fixed-bed studies, it is concluded that granular activated carbon is a technique that can be used for the removal of the fungicide carbendazim dissolved in aqueous matrices with NOM, which is usually present in sources that serve as water supplies for human consumption. This study contributed to a better understanding of the adsorption of carbendazim onto granular activated carbon, especially in continuous flow column tests.

DATA AVAILABILITY STATEMENT

All relevant data are included in the paper or its Supplementary Information.

CONFLICT OF INTEREST

The authors declare there is no conflict.

REFERENCES

Agência Nacional de Vigilância Sanitária – ANVISA. 2022 Reavaliação toxicológica – ANVISA inicia a reavaliação do Carbendazim. 2022. Available at: https://www.gov.br/anvisa/pt-br/assuntos/noticias-anvisa/2020/anvisa-inicia-a-reavaliacao-do-carbendazim (accessed 26 November 2022) (In Portuguese).

Ahmed, M. J. & Theydan, S. K. 2012 Adsorption of cephalexin onto activated carbons from *Albizia lebbeck* seed pods by microwave-induced KOH and K_2CO_3 activations. *Chem. Eng. J.* **211–212**, 200–207. https://doi.org/10.1016/j.cej.2012.09.089.

Allen, S. J., Mckay, G. & Khader, K. Y. H. 1989 Intraparticle diffusion of a basic dye during adsorption onto sphagnum peat. *Environ. Pollut.* **56**, 39–50.

Almeida, I. R., Silva, S. W., Tavares, L. C. & Benetti, A. D. 2023 Carbendazim adsorption on granular activated carbon of coconut shell: Optimization and Thermodynamics. *Revista AIDIS de Ingeniería y Ciencias Ambientales: Investigación, desarrollo y práctica* **16**(2), 456–476.

American Water Works Association (AWWA). 2005 *Water Treatment Plant Design*, 4th edn. United States, Denver, Colorado. McGraw-Hill, 972 p.

Anfar, Z., Ait Ahsaine, H., Zbair, M., Amedlous, A., Ait El Fakir, A., Jada, A. & El Alem, N. 2020 Recent trends on numerical investigations of response surface methodology for pollutants adsorption onto activated carbon materials: A review. *Crit. Rev. Environ. Sci. Technol.* **50**, 1043–1084. https://doi.org/10.1080/10643389.2019.1642835.

Cao, X., Han, H., Yang, G., Gong, X. & Jing, J. 2011 The sorption behavior of DDT onto sediment in the presence of surfactant cetyltrimethylammonium bromide. *Mar. Pollut. Bull.* **62**, 2370–2376. https://doi.org/10.1016/j.marpolbul.2011.08.035.

Carter, C. W. & Suffet, I. H. 1982 Binding of DDT to dissolved humic materials. *Environ. Sci. Technol.* **16**(11), 735–740.

Chemicalize. 2021 Carbendazim. Available at: https://chemicalize.com/app/search/Carbendazim (accessed 19 April 2021).

Coelho, E. R. C. & Rozário, A. 2019 Removal of 2,4-d in water samples by adsorption in fixed beds of granular activated carbon on reduced scale. *Eng. Sanit. Ambient.* **24**, 453–462. https://doi.org/10.1590/s1413-41522019182897.

Corwin, C. J. & Summers, R. S. 2010 Scaling trace organic contaminant adsorption capacity by granular activated carbon. *Environ. Sci. Technol.* **44**, 5403–5408. https://doi.org/10.1021/es9037462.

Crittenden, J. C., Hand, D. W., Arora, H. & Lykins, B. W. 1987 Design considerations for GAC treatment of organic chemicals. *J. Am. Water Work. Assoc.* **79**, 74–82. https://doi.org/10.1002/j.1551-8833.1987.tb02786.x.

Crittenden, J. C., Reddy, P. S., Arora, H., Trynoski, J., Hand, D. W., Perram, D. L. & Summers, R. S. 1991 Predicting GAC performance with rapid small-scale column tests. *J. Am. Water Works Assoc.* **83**, 77–87. https://doi.org/10.1002/j.1551-8833.1991.tb07088.x.

Crittenden, J. C., Trussel, R. R., Hand, D. W., Howe, K. J. & Tchobanoglous, G. 2012 *MWH's Water Treatment: Principles and Design*, 3rd edn. Wiley & Sons, Hoboken, NJ, 1901 p.

Davis, M. K. & Chen, G. 2007 Graphing Kendall's τ. *Comput Stat Data Anal.* **51**, 2375–2378.

de Boer, J. H., Lippens, B. C., Linsen, B. G., Broekhoff, J. C. P., van den Heuvel, A. & Osinga, T. J. 1966 Thet-curve of multimolecular N_2-adsorption. *J. Colloid Interface Sci.* **21**, 405–414. https://doi.org/10.1016/0095-8522(66)90006-7.

Dehghani, M. H., Karri, R. R., Lima, E. C., 2021 Adsorption: Fundamental aspects and applications of adsorption for effluent treatment. In: *Green Technologies for Defluoridation of Water*, 1st edn (Dehghani, M. H., Karri, R. R. & Lima, E. C., eds). Elsevier, Amsterdam, Chapter 3, 41–88 p.

Del Vecchio, P., Haro, N. K., Souza, F. S., Marcílio, N. R. & Féris, L. A. 2019 Ampicillin removal by adsorption onto activated carbon: Kinetics, equilibrium and thermodynamics. *Water Sci. Technol.* **79**, 2013–2021. https://doi.org/10.2166/wst.2019.205.

Domergue, L., Cimetière, N., Giraudet, S. & Cloirec, P. L. 2022 Adsorption onto granular activated carbons of a mixture of pesticides and their metabolites at trace concentrations in groundwater. *J. Environ. Chem. Eng.* **10**(5), 108218. https://doi.org/10.1016/j.jece.2022.108218.

Duan, J. & Gregory, J. 2003 Coagualtion by hydrolyzing metal salts. *Adv. Colloid Interface Sci.* **100–102**, 475–502. https://doi.org/10.1016/S0001-8686(02)00067-2.

Dulio, V., Von Der Ohe, P. C., Botta, F., Ipolyi, I., Ruedel, H. & Slobodnik, J. 2014 The NORMAN Network's Special View on Prioritisation of Biocides as Emerging Contaminants, 4–5.

Ersan, G., Kaya, Y., Apul, O. G. & Karanfil, T. 2016 Adsorption of organic contaminants by graphene nanosheets, carbon nanotubes and granular activated carbons under natural organic matter preloading conditions. *Sci. Total Environ.* **565**, 811–817. https://doi.org/10.1016/j.scitotenv.2016.03.224.

Giacomni, F., Menegazzo, M. A. B., da Silva, M. G., da Silva, A. B. & de Barros, M. A. S. D. 2017 Importância da determinação do ponto de carga zero como característica de tingimento de fibras proteicas. *Rev. Mater.* **22**, 2. https://doi.org/10.1590/S1517-707620170002.0159. (In Portuguese).

Guillossou, R., Le Roux, J., Mailler, R., Pereira-Derome, C. S., Varrault, G., Bressy, A., Vulliet, E., Morlay, C., Nauleau, F., Rocher, V. & Gasperi, J. 2020 Influence of dissolved organic matter on the removal of 12 organic micropollutants from wastewater effluent by powdered activated carbon adsorption. *Water Res.* **172**, 115487.

Guo, S., Zhong, S. & Zhang, A. 2013 Privacy-preserving Kruskal–Wallis test. *Comput Methods Programs Biomed* **112**(1), 135–145.

Haro, N. K., Del Vecchio, P., Marcilio, N. R. & Féris, L. A. 2017 Removal of atenolol by adsorption – study of kinetics and equilibrium. *J. Clean. Prod.* **154**, 214–219. https://doi.org/10.1016/j.jclepro.2017.03.217.

Haro, N. K., Dávila, I. V. J., Nunes, K. G. P., de Franco, M. A. E., Marcilio, N. R. & Féris, L. A. 2021 Kinetic, equilibrium and thermodynamic studies of the adsorption of paracetamol in activated carbon in batch model and fixed-bed column. *Appl. Water Sci.* **11**, 1–9. https://doi.org/10.1007/s13201-020-01346-5.

Hgeig, A., Novaković, M. & Mihajlović, I. 2019 Sorption of carbendazim and linuron from aqueous solutions with activated carbon produced from spent coffee grounds: Equilibrium, kinetic and thermodynamic approach. *J. Environ. Sci. Heal. – Part B Pestic. Food Contam. Agric. Wastes* **54**, 226–236. https://doi.org/10.1080/03601234.2018.1550307.

Ho, Y. S. & Mckay, G. 1998 A comparison of chemisorption kinetic models applied to pollutant removal on various sorbents. *Process Saf. Environ. Prot.* **76**, 332–340.

Hollander, M. & Wolfe, D. A. 1973 *Nonparametric Statistical Methods*. John Wiley & Sons, New York, pp. 115–120.

Jin, X., Ren, J., Wang, B., Lu, Q. & Yu, Y. 2013 Impact of coexistence of carbendazim, atrazine, and imidacloprid on their adsorption, desorption, and mobility in soil. *Environ. Sci. Pollut. Res.* **20**, 6282–6289. https://doi.org/10.1007/s11356-013-1657-2.

Kaduba, J. & Banza, M. 2020 Modification of clinoptilolite with dialkylphosphinic acid for the selective removal of cobalt (II) and nickel (II) from hydrometallurgical effluent. *Can. J. Chem. Eng.* **94**(1), 168–178.

Kempisty, D. M., Arevalo, E., Spinelli, A. M., Edeback, V., Dickenson, E. R. V., Husted, C., Higgins, C. P., Summers, R. S. & Knappe, D. R. U. 2022 Granular activated carbon adsorption of perfluoroalkyl acids from ground and surface water. *AWWA Water Sci.* **4**, 1–14. https://doi.org/10.1002/AWS2.1269.

Kendall, M. G. 1938 A new measure of rank correlation. *Biometrika* **30**, 81–93.

Kennedy, A. M., Reinert, A. M., Knappe, D. R. U., Ferrer, I. & Summers, R. S. 2015 Full- and pilot-scale GAC adsorption of organic micropollutants. *Water Res.* **68**, 238–248. https://doi.org/10.1016/j.watres.2014.10.010.

Kennedy, A. M., Reinert, A. M., Knappe, D. R. U. & Summers, R. S. 2017 Prediction of full-scale GAC adsorption of organic micropollutants. *Environ. Eng. Sci.* **34**, 496–507. https://doi.org/10.1089/ees.2016.0525.

Kümmerer, K., 2011 Emerging contaminants. In: *Treatise on Water Science*, 1st edn. (Wilderer, P. A., ed.). Elsevier, IWA, Amsterdam, pp. 69–87. doi:10.1016/B978-0-444-53199-5.00052-X.

Li, X., Zhou, Q., Wei, S., Ren, W. & Sun, X. 2011 Geoderma adsorption and desorption of carbendazim and cadmium in typical soils in northeastern China as affected by temperature. *Geoderm.* **160**, 347–354. https://doi.org/10.1016/j.geoderma.2010.10.003.

Li, G., Li, J., Tan, W., Yang, M., Wang, H. & Wang, X. 2022 Effectiveness and mechanisms of the adsorption of carbendazim from wastewater onto commercial activated carbon. *Chemosphere* **304**, 135231. https://doi.org/10.1016/j.chemosphere.2022.135231.

Liebscher, E. 2021 Kendall regression coefficient. *Comput. Stat. Data Anal.* **157**, 107140.

Lule, G. M. & Atalay, M. U. 2014 Comparison of fenitrothion and trifluralin adsorption on organo-zeolites and activated carbon. Part II: Thermodynamic parameters and the suitability of the kinetic models of pesticide adsorption. *Part. Sci. Technol.* **32**, 426–430. https://doi.org/10.1080/02726351.2014.892403.

Mavaieie Jr., P. A. & Benetti, A. D. 2021 Remoção de carbono orgânico dissolvido de águas filtradas com tratamento complementar por pré-oxidação com ozônio e adsorção em carvão ativado. *Eng. Sanit. Ambient.* **26**, 989–1001. (In Portuguese).

Mazellier, P., Leroy, É. & Legube, B. 2002 Photochemical behavior of the fungicide carbendazim in dilute aqueous solution. *J. Photochem. Photobiol. A Chem.* **153**, 221–227.

Metcalf and Eddy. 2014 *Wastewater Engineering – Treatment and Reuse*, 4th edn. McGraw-Hill, Boston, USA, 1408 p.

Miyittah, M. K., Tsyawo, F. W., Kumah, K. K., Stanley, C. D. & Rechcigl, J. E. 2016 Suitability of two methods for determination of point of zero charge (PZC) of adsorbents in soils. *Commun. Soil Sci. Plant Anal.* **47**, 101–111. https://doi.org/10.1080/00103624.2015.1108434.

Moussavi, G., Hosseini, H. & Alahabadi, A. 2013 The investigation of diazinon pesticide removal from contaminated water by adsorption onto NH_4Cl-induced activated carbon. *Chem. Eng. J.* **214**, 172–179. https://doi.org/10.1016/j.cej.2012.10.034.

Novotny, V. 2002 *Water Quality: Diffuse Pollution and Watershed Management*. Wiley, 888 p, Hoboken, New Jersey, United States.

Paszko, T. 2006 Sorptive behavior and kinetics of carbendazim in mineral soils. *Polish J. Environ. Stud.* **15**, 449–456.

Peduzzi, P. 2022 Anvisa proíbe uso do fungicida carbendazim em produtos agrotóxicos. Agência Brasil. 2022. Available at: https://agenciabrasil.ebc.com.br/saude/noticia/2022-08/anvisa-proibe-uso-do-fungicida-carbendazim-em-produtos-agrotoxicos (accessed 20 October 2022) (In Portuguese).

Pelekani, C. & Snoeyink, V. L. 1999 Competitive adsorption in natural water: Role of activated carbon pore size. *Water Res.* **33**, 1209–1219. https://doi.org/https://doi.org/10.1016/S0043-1354(98)00329-7.

Piccin, J. S., Cadaval, J. R., Pinto, T. R. S., de, L. A. A., Dotto, G. L., 2017 Adsorption isotherms in liquid phase: Experimental, modeling, and interpretations. In: *Adsorption Processes for Water Treatment and Purification*, 1st eds (Bonilla-Petriciolet, A., Mendoza-Castillo, D. I. & Reynel-Ávila, H. E., eds). Springer International Publishing, Cham, pp. 19–51.

Plattner, J., Kazner, C., Naidu, G. & Wintgens, T. 2018 Removal of selected pesticides from groundwater by membrane distillation. *Environ. Sci. Pollut. Research* **25**, 20336–20347. https://doi.org/10.1007/s11356-017-8929-1.

Rama, E. M., Bortolan, S., Leivas, M., Cristina, D., Gerardin, C. & Gastaldello, E. 2014 Reproductive and possible hormonal effects of carbendazim q. *Regul. Toxicol. Pharmacol.* **69**, 476–486. https://doi.org/10.1016/j.yrtph.2014.05.016.

Rizzi, V., Gubitosa, J., Fini, P., Romita, R., Agostiano, A., Nuzzo, S. & Cosma, P. 2020 Commercial bentonite clay as low-cost and recyclable 'natural ' adsorbent for the carbendazim removal/recover from water: Overview on the adsorption process and preliminary photodegradation considerations. *Colloids Surfaces A* **602**, 125060. https://doi.org/10.1016/j.colsurfa.2020.125060.

Ruiz, B., Cabrita, I., Mestre, A. S., Parra, J. B., Pires, J., Carvalho, A. P. & Ania, C. O. 2010 Surface heterogeneity effects of activated carbons on the kinetics of paracetamol removal from aqueous solution. *Appl. Surf. Sci.* **256**, 5171–5175. https://doi.org/10.1016/j.apsusc.2009.12.086.

Sellaoui, L., Gómez-Avilés, A., Dhaouadi, F., Bedia, J., Bonilla-Petriciolet, A., Rtimi, S. & Belver, C. 2023 Adsorption of emerging pollutants on lignin-based activated carbon: Analysis of adsorption mechanism via characterization, kinetics and equilibrium studies. *Chem. Eng. J.* **452**, 139399. https://doi.org/10.1016/j.cej.2022.139399.

Silanpää, M. 2015 *Natural Organic Matter in Water: Characterization and Treatment Methods*. Amsterdan: Elsevier/IWA, Amsterdam. https://doi.org/10.1016/C2013-0-19213-6.

Summers, R. S., Knappe, D. R. U. & Snoeyink, V. L., 2011 Adsorption of organic compounds by activated carbon. In: *Water Quality & Treatment: A Handbook on Drinking Water* (Edzwald, K. J., ed.). 6th edn, McGraw-Hill Education, Denver.

Thurman, E., Wershaw, R. L., Malcolm, R. L. & Pinckney, D. J. 1982 Molecular sizes of aquatic humic substances. *Org. Geochem.* **4**, 27–35. https://doi.org/10.1016/0146-6380(82)90005-5.

Voltan, P. E. N., Dantas, A. d. B., Paschoalato, C. F. R. & Di Bernardo, L. 2016 Predição da performance de carvão ativado granular para remoção de herbicidas com ensaios em coluna de escala reduzida. *Eng. Sanit. E Ambient.* **21**, 241–250. https://doi.org/10.1590/s1413-41522016138649.

Wang, T., Yu, C., Chu, Q., Wang, F., Lan, T. & Wang, J. 2020 Adsorption behavior and mechanism of five pesticides on microplastics from agricultural polyethylene films. *Chemosphere* **244**, 125491. https://doi.org/10.1016/j.chemosphere.2019.125491.

Water Resources Mission Area (WRMA). 2019 *Emerging Contaminants*. Available at: https://www.usgs.gov/mission-areas/water-resources/science/emerging-contaminants (accessed 2 May 2023).

Zhu, P., Sottorff, I., Zhang, T. & Helmreich, B. 2023 Adsorption of heavy metals and biocides from building runoff onto granular activated carbon – the influence of different fractions of dissolved organic matter. *Water* **15**(11), 2099. https://doi.org/10.3390/w15112099.

First received 18 July 2023; accepted in revised form 8 February 2024. Available online 1 March 2024